

Granitic Rocks of the Rio dos Bugres Mine: Host Rocks of Fluorite Deposits in Southernmost Brazil

J. A. FLORES, L. V. S. NARDI,¹ M. L. L. FORMOSO,

*Centro de Estudos em Geoquímica e Petrologia, Instituto de Geociências, Universidade Federal do Rio Grande do Sul,
Av. Bento Gonçalves 9500, C. P. 15011, 91501-970 Porto Alegre, RS, Brazil*

A. MEUNIER,

*Laboratoire de Hydrogéologie, Artilles, Sols et Altérations (UMR 6532),
Université de Poitiers, 40, avenue du Recteur Pineau, BP 633, 86022 Poitiers Cedex, France*

M. L. PASCAL,

Institut des Sciences de la Terre d'Orleans (CNRS-ISTO), 1A, rue de la Férollerie, F-45071 Orleans Cedex 02, France

M. FONTEILLES,

Laboratoire de Pétrologie, Université Pierre-et-Marie-Curie, 4 place Jussieu, F-75252 Paris Cedex 05, France

AND A. C. FERREIRA

*Centro de Estudos em Geoquímica e Petrologia, Instituto de Geociências, Universidade Federal do Rio Grande do Sul,
Av. Bento Gonçalves 9500, C. P. 15011, 91501-970 Porto Alegre, RS, Brazil*

Abstract

Most fluorite deposits in southernmost Brazil are hosted by Neoproterozoic granitic associations. Fluorite deposits are, nevertheless, much younger than granitic magmatism, and the only probable role of granitic rocks in fluorite genesis was as a source of F. This paper characterizes granitic-dioritic associations in which these fluorite lodes and veins are localized. The granitic suite includes quartz diorites, tonalites, biotite-bearing syenogranites, monzogranites, and rhyolite dikes. It is interpreted as formed by partial mixing of basic and granitic melts, generating hybrid products, such as the tonalitic rocks. The granitic magmatism is correlated with the late-transcurrent magmatism that characterizes the post-collisional stages of the Brasiliano-Pan-African orogenic cycle in southernmost Brazil. Basic rocks have mildly alkaline or continental tholeiitic affinities. The associated granitic magmatism was probably produced by crustal melting or, alternatively, as a reaction product of mantle-derived basic melts with quartz-feldspathic gneissic crustal sequences. Trace-element and REE patterns of the basic rocks are consistent with melts produced from a mantle previously modified by subduction-related metasomatism. The granitic rocks show trace-element compositions compatible with comagmatic products derived from the basic magmatism, which can also be interpreted as an effect of mixing between two non cogenetic magmas. Hydrothermally altered granites exhibit HREE-enriched patterns that can be used as a prospective tool for fluorite deposits.

Introduction

THE MOST IMPORTANT fluorite deposits in South America are in Santa Catarina State, southern Brazil (Fig. 1). Fluorite ores are post-Cretaceous in age and their host rocks are mainly Neoproterozoic granitic rocks of the so-called Pedras Grandes suite (Sallet, 1988). The age of fluorite mineralization was estimated from K-Ar data in hydrothermally

altered host rocks (Tassinari and Flores, 1992) and from fission tracks on apatites from the host granitoids (Jelinek, 2002), producing ages that range from 130 to 45 Ma. Most genetic studies have concluded that the fluorine source for hydrothermal solutions was fluorite disseminated in older hydrothermally modified zones in the Neoproterozoic granitic rocks (Sallet, 1988; Bastos Neto et al. 1996; Jelinek, 2002; Flores, 1998). The Rio dos Bugres fluorite mine is an example of such deposits in these fertile granites. A subsolidus hydrothermal

¹Corresponding author; email: lauro.nardi@ufrgs.br

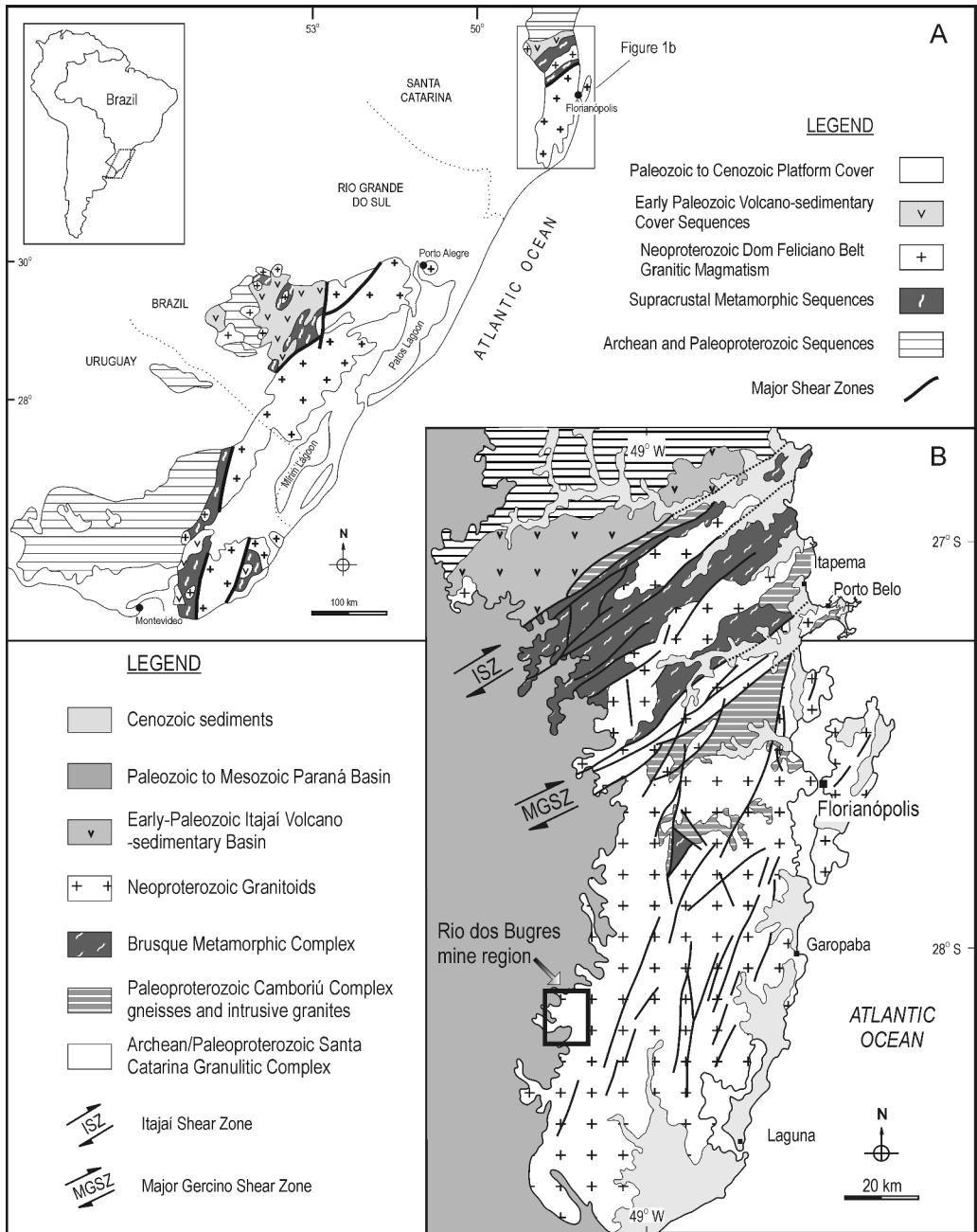


FIG. 1. Main geological features of southernmost Brazil and the studied area of Rio dos Bugres Mine region (modified from Bitencourt and Nardi, 2004).

event is registered in the granitic rocks, leading mainly to sodic and potassic alterations (Flores, 1998). In this paper, the main geological, petro-

graphic, and geochemical features of Rio dos Bugres Mine magmatic rocks are presented and discussed.

The rock section of the Rio dos Bugres mine is part of the Dom Feliciano belt, which encompasses deformed granitoids, migmatites, metasedimentary rocks, molassic sedimentary and volcanic acid rocks, and a large amount of late and post-tectonic granitoids (Fragoso-César et al., 1982). Most granitoids have ages in the range 640–590 Ma, and were emplaced during the development of the Southern Brazilian shear belt (Bitencourt and Nardi, 1993), a major translithospheric transcurrent belt composed of several anastomosing, km-wide shear zones, related to the post-collisional period of the Brazilian-Pan African cycle. The early stages of the transcurrent event are associated with basic magmatism of continental tholeiitic affinity, coeval granitoids compositionally similar to high-K calc-alkaline rocks. This magmatism was followed by a shoshonitic one and eventually, the late-stages of transcurrent were associated with basic magmatism of mildly alkaline affinity and coeval sodic alkaline metaluminous granitic rocks (Bitencourt and Nardi, 1993, 2000). Except for the leucogranites, basic magmatism is associated with all kinds of granite associations as mafic microgranular enclaves, dikes, and small intrusions. Comingling and composite dikes, involving basic and acid rocks, are particularly abundant in the latest magmatism.

The magmatism related to the early stages of transcurrent (~640 Ma) shows geochemical signatures similar to those of mature magmatic arc rocks, whereas the late-transcurrent rocks (~590 Ma) show compositions closer to rocks of within-plate settings, probably derived from OIB mantle sources (Bitencourt and Nardi, 2000; Sommer et al., 2005).

Leucogranites, biotite granites, tonalites, and quartz diorites are the dominant lithologies in the Rio dos Bugres mine region. Some of them exhibit effects of the late stages of transcurrent deformation, locally resulting in mylonite formation. According to structural evidence, these granitoids are late-transcurrent, and deformation is confined to shear zones of a few meters width. The presence of comingling features, similar structural patterns, and abundant diffuse contacts suggest that dioritic and granitic rocks were probably coeval. Both parental magmas interacted in different ways, generating homogeneous and heterogeneous mixing products. Tonalitic rocks were probably produced by homogeneous mixing, whereas mafic microgranular enclaves in granitoids and synplutonic dikes are evidence of heterogeneous mixing. Rhyolite dikes crosscut these granitoids, but are probably related to the

same magmatic event. Subsidiary hydrothermal alteration led to the formation of apogranites and albitites with secondary albite and lower proportions of muscovite, at temperatures of about 400–450°C (Flores, 1998). Albitization was followed by propylitization at lower temperatures. According to apatite fission track age determinations for the host granitoids (Jelinek, 2002), fluorite deposits formed a long time (about 500 m.y.) afterwards, by percolation of hydrothermal fluids through reactivated fractures along older shear zones (Flores, 1998).

Petrography and Mineral Chemistry

Fifteen samples were selected from rocks least affected by deformational or hydrothermal processes, and modal values were plotted in the QAP diagram. Major minerals were analysed by microprobe—Cameca SX 50 (15 kV, 4 nA) in the Université Pierre et Marie Curie, Paris. Two groups were identified, a more mafic one with quartz diorites and tonalites, and a felsic one with monzogranites and syenogranites.

Tonalites and quartz diorites show an oriented fabric controlled by magmatic flow defined by plagioclases, amphiboles, and biotites. Textures are medium to coarse grained, granitic, and locally sub-graphic. The primary mineralogy is composed of zoned plagioclase and amphibole, late crystallized alkali feldspar with inclusions of biotite, quartz, ilmenite, magnetite, apatite, and zircon. Imbrications of plagioclase, amphibole, and biotite are the most evident deformational features. Simplectic intergrowths of amphibole and quartz are interpreted as a result of magmatic reactions, probably on primary pyroxenes. Secondary minerals are widespread in the tonalitic and quartz dioritic rocks; they include chlorite, corrensite, actinolite, epidote, albite, white mica, carbonates, and alkali feldspar.

The felsic rocks are monzo- and syenogranites with an oriented fabric parallel to that of tonalitic and quartz dioritic rocks, which is more intense close to mylonitic zones. The foliation of monzogranites is generally defined by biotite orientation. Along high-stress zones a few meters wide, feldspar is replaced by white mica, quartz ribbons are formed, and a mylonitic fabric is developed parallel to the host granite foliation. Primary textures are generally granitic, medium to coarse grained, and the major minerals are oligoclase, microcline, quartz, and biotite. Chlorite, white mica, carbonate, and epidote are the most abundant secondary

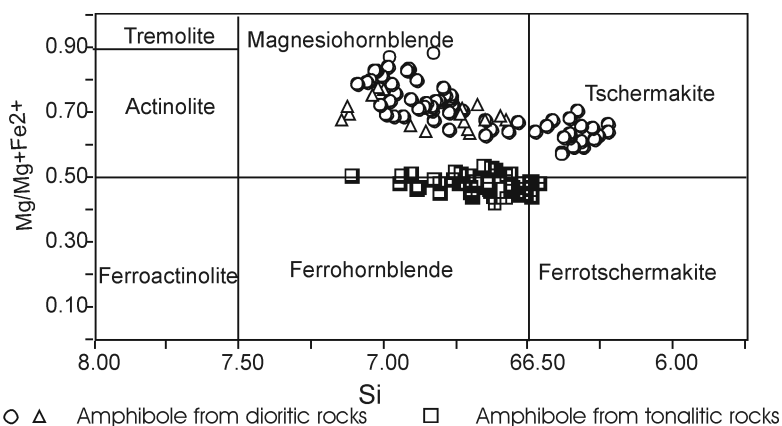


FIG. 2. Amphibole classification (Leake et al., 1997) shows two groups of amphiboles with distinct $\text{FeO}/\text{FeO} + \text{MgO}$ ratios in the Mina Rio dos Bugres granitoids.

minerals in the monzogranites. Syenogranites are leucocratic, with medium- to coarse-grained granitic texture, and with an isotropic to moderately oriented fabric, defined by orientation of micas. Pegmatitic and graphic textures are abundant. They are constituted mostly by euhedral to subhedral microcline, albitic plagioclase, biotite, generally replaced by white mica, and late crystallized quartz. The secondary mineralogy is mainly white mica, chlorite, epidote, and carbonate. Mylonitic textures are similar to those observed in monzogranites. Rhyolite dikes crosscut the mafic and felsic rocks.

Magmatic amphibole composition was determined by microprobe in five samples of quartz diorite and tonalite and their classification was based on Leake et al. (1997). Fe^{+++} was calculated according to the procedure of Droop (1987). Two groups of amphiboles, with different proportions of Mg/Fe^{++} , were observed (Fig. 2): magnesianhornblende to tschermakite and ferrohornblende-magnesianhornblende to ferrotschermakite. The former group occurs in the less differentiated diorites and is typically composed of poikilitic grains with biotite inclusions, whereas the second occurs in the more differentiated tonalites, generally as euhedral grains with sharp contacts with biotite. Magnesianhornblende is mostly altered to biotite or secondary actinolite. $\text{Mg}/(\text{Mg} + \text{Fe}^{++})$ ratio varies in each group from 0.57 to 0.75 and from 0.42 to 0.56, respectively. The presence of these distinct groups of amphiboles (Fig. 2) suggests that quartz diorites and tonalites

crystallized from different liquids, under different oxidation conditions, and do not represent the single evolution in a closed system. The Al content in magnesian and ferrohornblende is relatively high, and suggests they were crystallized under pressures close to 2–3 kbar according to the curves suggested by Anderson and Smith (1995) for temperatures about 700°C.

Biotite is present in tonalite as subhedral grains, generally associated with amphiboles, and in places altered to chlorite. In monzogranites and syenogranites, biotite is generally transformed to white mica and presents greenish pleochroism, and its composition reflects these transformations. $\text{MR}^3\text{R}^3\text{R}^2$ diagram (Velde, 1985) shows three compositional groups of micas and different alteration trends of biotite from tonalites and biotites from monzo- and syenogranites. $\text{Fe}/(\text{Fe} + \text{Mg})$ ratios in the biotite from tonalites vary from 0.4 to 0.6 and are equivalent to those of amphibole, confirming their simultaneous crystallization under magmatic conditions. Mg and Al contents are comparable to those found in biotites of biotite \pm amphibole \pm pyroxene granites of sub-alkaline series according to Nachit et al. (1985).

Plagioclase of tonalites shows euhedral to subhedral forms and varies from An_{34} to An_{57} ; in the monzonites it is in the range An_{12-28} , and in the syenogranites it has a composition close to albite. Alkali feldspar is compositionally very close to the Or apex in the An-Ab-Or diagram, with Ab contents under 20% and An lower than 5%.

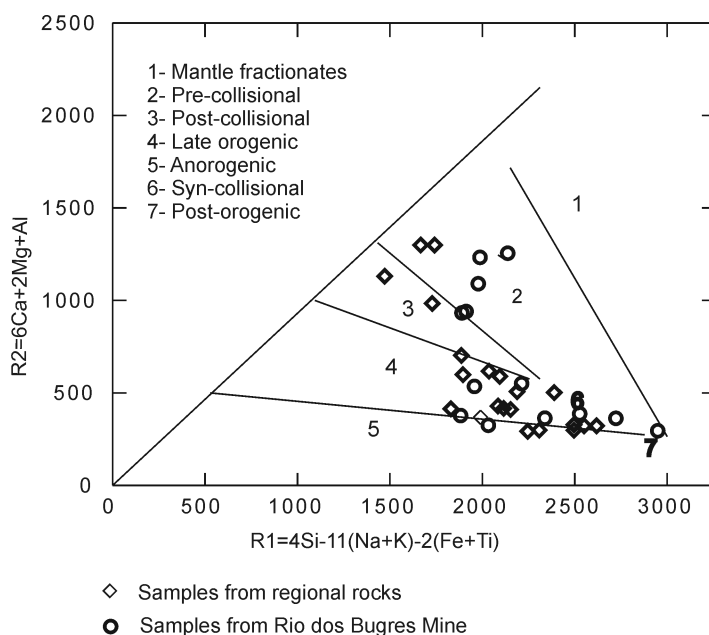


FIG. 3. Samples of Rio dos Bugres Mine granitoids in the R1R2 diagram with the fields suggested by Batchelor and Bowden (1985).

Bulk-Rock Geochemistry

Forty-two samples of granitic and quartz dioritic rocks of the Rio dos Bugres mine region were selected for major- and trace-element determinations (Table 1). Mylonitic granitoids and albitized granites were included among the selected samples in order to control the compositional variations caused by mylonitization and hydrothermalism.

The granitic samples were plotted in the cationic diagram P ($K/(Na+Ca)$) versus Q ($Si/3 - (K+Na+2Ca/3)$) suggested by Debon et al. (1988), and were classified mostly as syenogranites and monzogranites, including also granodiorites and quartz diorites. The results are very similar to those obtained through modal determinations plotted in the QAP diagram. These same parameters also discriminate mylonitic and hydrothermally altered rocks, plotted in the right superior corner of this diagram. On the other hand, albitized samples plot in the lower part of the Q versus P diagram. This effect of albitization is reflected in increased contents of normative albite.

The R1 ($4Si - 11(Na+K) - 2(Fe+Ti)$) versus R2 ($6Ca + 2Mg + Al$) cationic diagram, with the fields suggested by Batchelor and Bowden (1985), shows the studied samples assembled in three distinct

groups (Fig. 3). Quartz dioritic rocks have higher values of R2, some granitoid samples plot in a field typical of high-potassium granitoids, and the others are localized close to the border of the anorogenic granite field, which is considered the field of metaluminous granites of alkaline association by Nardi (1991).

The studied samples plot close to the boundary of subalkaline and silica-saturated alkaline rocks in the TAS diagram (Fig. 4), for plutonic rocks (Middlemost, 1994). Intermediate rocks are subalkaline, high-K rocks evolving to more alkaline acid compositions, in some cases with K_2O/Na_2O ratios reaching values higher than 2.

Molecular proportions of alkalis and alumina indicate that these granitoids are mostly metaluminous, with peraluminous types among the two-mica bearing granites and the leucocratic syenogranites. Albitized rhyolites and albitites have $(Na_2O + K_2O)$ about 12 wt% and show peraluminous to metaluminous natures. Mylonite generation along shear zones, increase the peraluminous character of protoliths, and cause Na and Ca depletion.

The distribution of samples in the diagrams FeO_T/MgO or $(K_2O + Na_2O)/CaO$ versus $(Zr + Nb + Ce + Y \text{ ppm})$ proposed by Whalen et al. (1987)

TABLE I. Major (wt%) and Trace Element (ppm) Contents of Samples from Rio dos Bugres Mine Rocks

Sample	SiO ₂	TiO ₂	Al ₂ O ₃	Fe ₂ O ₃	FeO	MnO	MgO	CaO	Na ₂ O	K ₂ O	P ₂ O ₅	LOI	Total
GCB-02	75.60	0.17	12.60	0.73	0.42	0.03	0.04	0.53	3.90	4.90	0.03	0.81	99.69
GCB-29-A	75.30	0.05	13.00	0.17	0.84	0.02	0.07	0.47	4.50	4.80	0.03	0.54	99.77
GDM-40	70.60	0.29	14.80	0.05	1.70	0.05	0.52	0.99	3.30	6.00	0.24	1.20	98.99
GDM-58	72.80	0.15	14.60	0.05	1.10	0.04	0.43	0.95	4.60	4.70	0.09	0.51	99.87
GDM-72	71.40	0.21	14.30	0.44	1.40	0.04	0.52	1.00	3.30	6.00	0.21	0.83	98.81
GDM-74	71.70	0.29	13.90	0.26	1.30	0.03	0.53	0.68	3.30	6.70	0.24	0.95	99.32
N223-38,00	65.40	0.70	14.60	0.92	3.66	0.14	0.62	2.34	2.30	3.86	0.23	3.47	98.15
PG-35	67.20	0.54	15.10	0.90	2.70	0.07	0.92	2.20	3.70	4.80	0.16	1.46	99.15
PG-67	68.80	0.42	14.90	1.00	1.70	0.06	1.10	2.30	4.00	4.30	0.17	1.00	99.05
PG-68	70.10	0.39	14.20	0.55	2.20	0.06	0.63	1.90	3.60	4.80	0.16	1.20	99.04
PG-69	68.30	0.50	14.50	0.88	2.70	0.07	0.80	2.50	3.60	4.80	0.17	0.99	99.23
PG66	65.80	0.62	15.70	1.60	2.20	0.08	1.7	3.10	4.4	3.5	0.23	0.91	99.04
QD-55	54.30	1.00	15.40	1.30	8.00	0.14	5.90	6.70	3.10	2.10	0.21	1.55	98.90
QD-56	51.80	2.30	16.70	2.20	8.60	0.16	2.90	7.80	2.60	2.10	0.86	1.86	99.66
QD-57	55.50	1.60	16.70	2.90	5.30	0.10	3.50	5.90	3.80	2.40	0.53	1.34	99.28
QD-64	50.00	1.80	15.90	2.10	7.50	0.11	4.70	6.70	3.30	2.50	0.35	4.73	99.48
QD-80	60.60	1.10	16.50	1.90	3.90	0.09	2.80	4.80	4.60	2.00	0.36	1.19	99.65
RB11-12,60	72.10	0.17	14.00	0.16	0.79	0.02	0.24	0.82	2.77	6.24	0.20	1.64	98.20
RB11-14,35	75.20	0.16	12.40	0.36	0.76	0.02	0.25	0.95	2.53	5.80	0.08	1.05	99.44
RB11-19,35	52.40	1.17	12.50	1.85	6.42	0.18	7.62	5.85	1.35	3.32	0.12	4.81	97.40
RB11-44,85	55.00	1.37	15.70	2.18	6.37	0.16	3.32	5.73	2.38	2.39	0.28	3.95	98.61
RB11-54,20	55.60	.124	15.50	2.00	5.90	0.16	3.07	5.65	2.47	2.51	0.23	4.47	97.48
RB11-70,50	70.40	0.15	14.70	0.32	0.79	0.02	0.21	0.51	2.64	7.78	0.07	1.04	98.74
RB11-74,08	76.70	0.24	11.60	0.00	0.47	0.00	0.06	0.51	2.78	4.85	0.11	0.77	97.62
RB46-30,00	75.60	0.04	13.00	0.14	0.66	0.01	0.04	0.15	3.79	4.79	0.03	0.89	98.34
RB46-77,71	65.60	0.66	14.10	1.00	3.32	0.07	0.67	2.05	2.70	4.47	0.21	3.78	98.53

RB11-92,25	65.60	0.05	19.10	0.00	0.66	0.01	0.15	0.40	7.44	4.05	0.06	0.89	98.41
RB11-98,50	68.50	0.05	14.50	0.77	0.39	0.06	0.05	1.62	1.72	10.20	0.04	1.25	99.07
RB11-99,64	66.80	0.06	18.90	0.00	0.44	0.00	0.06	0.29	5.91	6.64	0.05	0.72	99.87
RB223-3,35	71.80	0.17	13.70	0.00	1.00	0.03	0.20	1.07	2.19	6.17	0.25	2.12	98.70
RB223-5,6,20	72.10	0.10	14.50	0.00	0.68	0.01	0.10	0.54	2.53	7.94	0.08	0.87	98.77
RB46-94,40	68.30	0.41	13.20	0.27	1.73	0.03	0.47	2.13	2.85	6.28	0.17	2.57	98.38
RB46-99,12	59.70	1.20	15.70	2.29	4.69	0.10	2.90	1.38	0.72	3.33	0.34	7.16	99.28
RB6-5,55	64.50	0.38	18.60	1.58	0.09	0.06	0.13	0.32	4.98	7.29	0.13	1.35	99.25
RB6-77,44	58.80	1.14	15.90	1.87	5.14	0.14	3.08	4.47	3.03	3.03	0.28	2.83	99.52
RB6-79,60	58.80	1.02	16.30	1.91	4.96	0.14	2.74	4.41	3.06	2.89	0.29	3.79	100.12
RB6-81,20	59.20	1.18	16.50	2.38	4.61	0.52	1.52	0.80	0.03	3.10	0.29	7.63	97.52
RB8-48,64	53.60	1.52	13.90	3.00	5.98	0.14	4.67	7.15	2.06	1.86	0.23	4.29	98.10
RIOL-4	75.60	0.06	12.70	0.21	0.98	0.05	0.03	0.54	4.40	4.90	0.03	0.48	99.79
RIOL-1	75.90	0.11	12.20	0.18	1.10	0.03	0.08	0.63	3.60	5.30	0.03	0.75	99.63
RIOL-2	75.20	0.12	12.10	0.26	1.30	0.03	0.20	0.82	3.50	5.30	0.03	0.92	99.22
RIOL-3	75.60	0.16	12.00	0.34	1.40	0.04	0.17	0.78	3.30	5.30	0.03	0.86	99.24

Table continues

TABLE 1. (continued) Trace Elements

Sample	Ba	Rb	Y	Zr	Nb	Pb	Ga	Ni	Sr	V	Cr	La	Ce	Nd	Sm	Eu	Dy	Yb
GCB-02	10	730	116	100	44	86	30	3	5	29	11	9.90	26.60	20.90	8.60	0.18	15.30	12.90
GCB-29-A	27	720	150	74	47	67	32	10	5	65	5	9.30	32.55	23.88	9.61	0.10	18.66	13.83
GDM-40	420	300	24	180	14	30	20	20	69	64	13							
GDM-58	320	260	30	54	14	41	18	11	140	44	24	12.90	31.13	14.31	3.20	3.20	2.83	1.56
GDM-72	420	270	13	125	14	66	19	7	72	18	7	42.04	105.90	46.24	7.75	0.77	2.60	0.85
GDM-74	440	350	13	135	10	23	8	9	140	46	10	45.02	110.00	47.47	8.02	0.78	2.75	0.93
N223-38,00	816	373	15	239	10	8	20	2	140	64	2	37.10	97.20	35.80	7.56	1.40	3.10	1.03
PG-35	830	190	47	99	15	15	18	7	160	40	3	49.10	115.40	50.79	9.48	1.55	6.90	3.38
PG-67	670	160	22	120	15	27	18	18	270	71	18	25.34	58.09	25.84	4.94	0.95	3.34	1.48
PG-68	650	210	56	200	17	23	17	16	110	55	100	41.47	97.14	42.68	7.71	1.21	6.34	3.63
PG-69	860	160	68	235	14	15	18	18	120	83	6	46.43	110.40	50.93	9.72	1.58	7.93	3.89
PG66	770	190	52	115	27	15	20	18	340	72	31	35.58	85.10	39.74	7.70	1.34	5.78	3.30
QD-55	560	81	74	120	5	44	23	95	300	210	130	24.11	49.1	28.70	6.15	1.47	5.76	2.69
QD-56	510	79	86	115	56	30	31	46	240	305	7	35.12	86.51	47.37	9.37	2.11	7.13	3.19
QD-57	790	56	40	140	5	30	22	57	480	170	62	33.19	86.80	44.41	8.56	2.06	4.27	1.62
QD-64	280	150	35	44	22	35	26	54	300	225	56	12.66	37.27	27.18	6.29	1.57	3.87	1.23
QD-80	670	110	27	145	20	5	21	63	480	150	49							
RB11-12.60	443	418	17	92	18	51	19	1	109	15	1	16.50	40.10	16.50	4.28	0.60	2.68	1.23
RB11-14.35	281	313	13	112	11	41	15	2	109	11	3	15.30	41.80	17.40	4.33	0.58	2.07	0.80
RB11-19.35	612	238	29	137	10	14	18	137	246	169	430	15.60	39.20	22.80	7.24	1.39	5.45	2.67
RB11-44.85	560	204	34	200	13	11	19	9	285	155	9	26.20	64.00	28.80	7.75	1.72	6.42	3.23

RB11-54,20	577	.269	34	198	11	14	19	9	269	145	11	24.10	60.50	25.60	6.70	1.58	6.36	3.36
RB11-70,50	430	509	21	92	10	50	17	2	109	11	2	19.60	53.30	20.50	5.32	0.63	2.98	1.60
RB11-74,08	402	471	20	119	21	21	13	0	80	12	6	21.60	55.20	23.50	5.90	0.63	3.47	1.32
RB11-92,25	186	512	148	137	56	25	35	0	69	9	2	7.33	26.90	17.80	9.35	0.20	20.70	14.50
RB11-98,50	544	1037	219	164	59	49	24	1	46	18	1	20.50	73.30	41.10	18.40	0.19	33.30	21.40
RB11-99,64	231	763	188	156	58	35	33	0	50	11	1	14.30	51.20	29.30	12.10	0.19	25.70	19.10
RB223-31,35	223	359	17	79	14	35	19	5	79	13	8	14.20	40.40	14.70	3.32	0.47	2.62	1.12
RB223-56,20	200	516	16	71	11	63	17	6	97	6	4	10.40	24.90	9.39	2.23	0.59	2.54	1.50
RB46-30,00	617	835	149	132	48	48	33	1	8	4	1	8.69	33.00	17.30	7.38	0.09	21.30	14.90
RB46-77,71	863	373	53	253	14	23	18	3	146	59	2	32.90	84.00	33.80	7.53	1.60	7.63	4.21
RB46-94,40	973	427	21	261	12	21	17	3	124	31	1	62.30	159.00	57.70	7.84	1.23	3.21	1.62
RB46-99,12	532	370	28	208	19	19	22	12	61	125	1	33.60	82.30	34.00	7.53	1.52	4.77	2.25
RB6-5,55	356	813	40	132	22	18	28	5	18	23	13	10.00	27.60	14.80	4.09	0.58	5.37	2.58
RB6-77,44	701	228	28	121	15	15	19	13	299	135	3	19.2	59.8	28.7	7.14	1.46	5.27	2.35
RB6-79,60	649	244	30	164	15	17	19	12	317	127	1	24.70	69.20	31.90	7.38	1.46	5.41	2.33
RB6-81,20	510	320	44	208	20	11	22	15	20	125	11	32.60	81.40	37.00	9.36	1.99	8.46	3.24
RB8-48,64	690	139	20	104	9	11	17	35	409	270	75	16.10	41.60	23.70	6.26	1.44	3.91	1.72
RIOL-4	260	270	40	97	25	30	17	10	18	50	9	18.48	48.93	26.71	6.84	0.67	6.90	3.95
RIOL-1	110	320	95	190	67	30	20	15	5	54	17	64.85	157.80	73.23	15.53	0.59	12.57	6.89
RIOL-2	130	350	110	140	22	30	19	17	19	48	12	88.49	210.50	97.76	20.06	0.76	16.05	8.14
RIOL-3	100	340	90	185	30	25	21	17	22	60	14	85.87	201.90	87.06	17.00	0.66	12.88	7.17

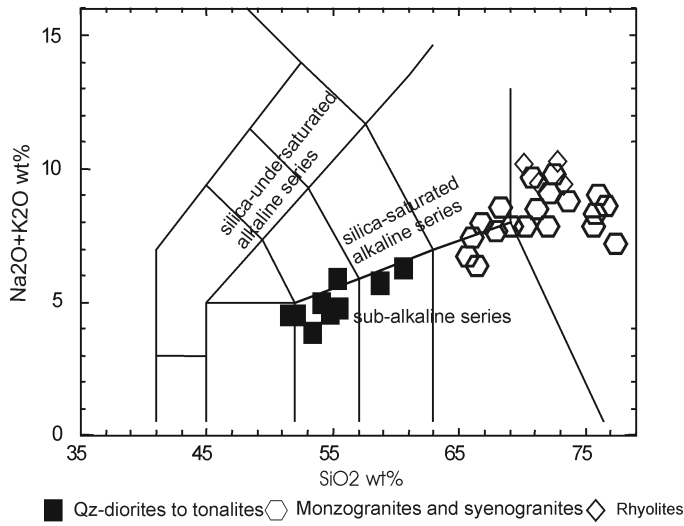


FIG. 4. Samples of Rio dos Bugres Mine granitoids in the TAS diagram (Le Maitre, 1989).

suggests the relationship of this magmatism with sources affected by subduction, such as those of magmatic-arc or post-collisional associations, evolving to alkaline with within-plate compositional features. The same trend is observed in the Nb versus Y and (Nb + Y) versus Rb diagrams (Fig. 5; Pearce et al., 1984; Pearce, 1996), where the post-collisional character of this magmatism is indicated. Rhyolite dike samples plot as typical products of within-plate magmatism.

Chondrite-normalized REE patterns (Sun, 1982) (Figs. 6 and 7) are similar for the major part of this magmatism, except for the more alkaline compositions, which show higher Yb values ($Yb_N \sim 20-40$) and more intense negative-Eu anomalies ($Sm_N/Eu_N \sim 10$). Positive Eu anomalies are observed in some samples with cumulative feldspar. Quartz-dioritic rocks present patterns with slight LREE to HREE fractionation ($Ce_N/Yb_N \sim 7$) and small negative Eu-anomalies ($Sm_N/Eu_N \sim 2$), which are similar to those of high-K calc-alkaline magmas from evolved continental arcs or from post-collisional settings. Similar REE patterns are also found in continental tholeiitic rocks related to post-collisional settings, where the magma sources still preserve the effects of subduction-related metasomatism. In the more differentiated monzogranites, the REE patterns preserve the same characteristics, with slight LREE enrichments and increase in the negative Eu anomalies. Syenogranites, locally with secondary muscovite, have REE patterns resembling those of

monzogranites, although with lesser amounts of REE. The syenogranite samples from Rio dos Bugres mine region show significant depletion of LREE. Rhyolite dikes are REE enriched relative to the previously described rocks, with intense negative Eu anomalies and slight fractionation of LREE to HREE. Such REE patterns have been described in acid alkaline volcanic or plutonic rocks with high fluorine contents or from within-plate settings (Bowden and Kinnaird, 1984).

The geochemical features of basic and acid rocks are common in the post-collisional silica-saturated alkaline magmatism, referred by several authors in the southern Brazil region (Nardi and Bonin, 1991; Bittencourt and Nardi, 1993). Albitization leads to REE patterns with no fractionation of LREE to HREE, with Ce_N and Yb_N values varying from 10 to 100, and very deep negative Eu anomalies.

Spidergrams with incompatible elements normalized against the theoretical ocean-ridge granite (Pearce et al., 1984) also illustrate the similarity of granitic rocks from Rio dos Bugres mine region and granitoids from mature continental arcs or from post-collisional settings (Fig. 8). The low LREE/Nb ratios of these magmatic rocks indicate their derivation from sources affected by previous subduction (Thompson et al., 1984).

The representation of major-element oxides against SiO₂ shows linear trends for compatible elements such as CaO, MgO and FeO, whereas Al₂O₃, Na₂O, and P₂O₅ show patterns that indicate strong

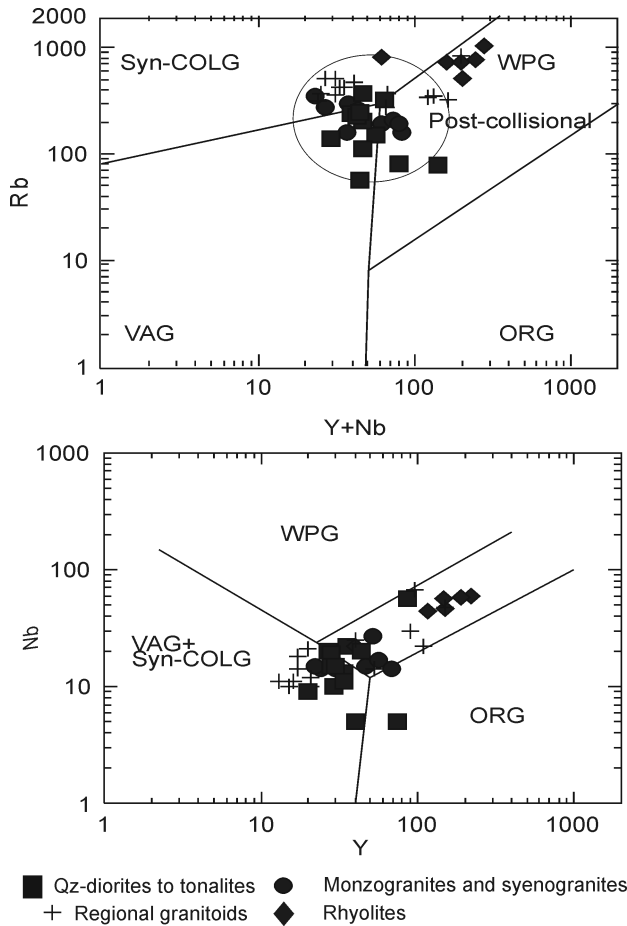


FIG. 5. Samples of Rio dos Bugres Mine granitoids in the Rb × Y + Nb and Y × Nb diagrams of Pearce et al. (1984) and Pearce (1996).

enrichment in the more contaminated mafic rocks, like those observed in contaminated mafic microgranular enclaves (Nardi and Lima, 2000) produced by mingling of compositionally contrasting magmas. Quartz-diorites and tonalites have geochemical features that suggest they represent hybridized dioritic magmas, probably due to partial mixing with granitic melts.

The distinct geochemical features of rhyolite dikes, mainly the higher HREE, Nb, Y, and alkali-element contents, result in a more prominent alkaline and within-plate character, observed in the latest magmatism associated with the transcurrent post-collisional tectonics in southern Brazil (Nardi and Bonin, 1991; Bitencourt and Nardi 1993).

Final Considerations

Basic and acidic magmas, presently represented by quartz-diorite-tonalite and granite-pegmatite-aplite associations, were simultaneously emplaced during the late stages of transcurrent events, related with the post-collisional stages (Liégeois, 1998) of the Brasiliano-Pan-African cycle, in the Rio dos Bugres mine region, southern Brazil. Partial mixing produced mainly hybrid tonalitic to quartz dioritic rocks. Structural patterns are consistent with late-transcurrent magmatism, where most fabrics were formed by magmatism flow controlled by transcurrent tectonic, and solid-state deformation is mostly localized along narrow shear

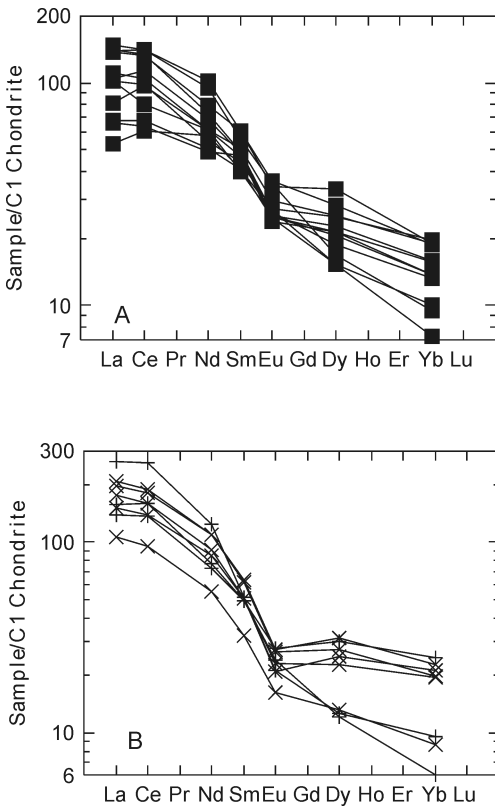


FIG. 6. REE chondrite-normalized patterns of dioritic (A) and tonalitic granitoids (B) from Rio dos Bugres Mine granitoids.

zones. Mylonites were produced along these narrow high-stress zones with thickness of up to a few meters.

The less differentiated rocks of this region are diorites and quartz diorites, whose trace-element compositions are similar to those of mildly alkaline basic rocks from the postcollisional Zimbros Intrusive Suite (Bitencourt and Nardi, 1993) and to low-TiO₂ basalts from the Paraná Basin (Peate et al., 1988).

The basic magmatism in the Rio dos Bugres mine region shows a mildly alkaline silica-saturated affinity, also comparable to continental tholeiitic (CFB-type) magmatism, with a variable contamination by granite melts, which modified their mineralogical and chemical composition. The compositional similarity of the studied quartz dioritic rocks with low-TiO₂ basalts from Paraná Basin magmatism is interpreted as evidence that both were

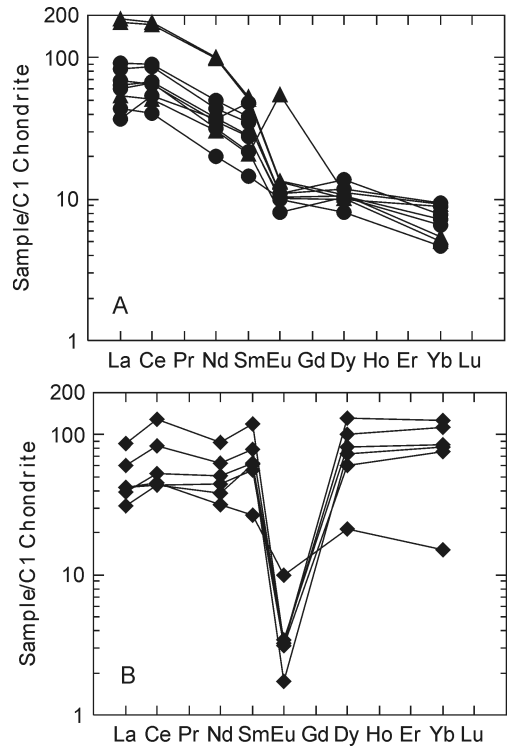


FIG. 7. REE chondrite-normalized patterns of granites (A) and albitized granites (B) from Rio dos Bugres Mine granitoids.

derived from similar mantle sources, as previously suggested by Bitencourt and Nardi (1993) for Neoproterozoic basic rocks from the Zimbros Intrusive Suite in the Porto Belo region. Granite melts have compositions consistent with melts derived from orthogneissic sequences, or may have been generated from reaction of mildly alkaline basic magmas with the metamorphic basement. Such a petrogenetic model was suggested by Patiño Douce (1995) and seems particularly suitable for high-K granites of tholeiitic affinity. Intermediate rocks were interpreted as produced from hybrid magmas generated by mixing.

The consistency of trace-element and REE patterns of basic and granitic rocks suggests that they can have a genetic relationship, which could be explained by the model of reaction between mantle basic melts and crustal metamorphic sequences developed by Patiño-Douce (1995, 1999). Geochemical patterns for major and trace elements are distinct for relatively unaltered and albitized

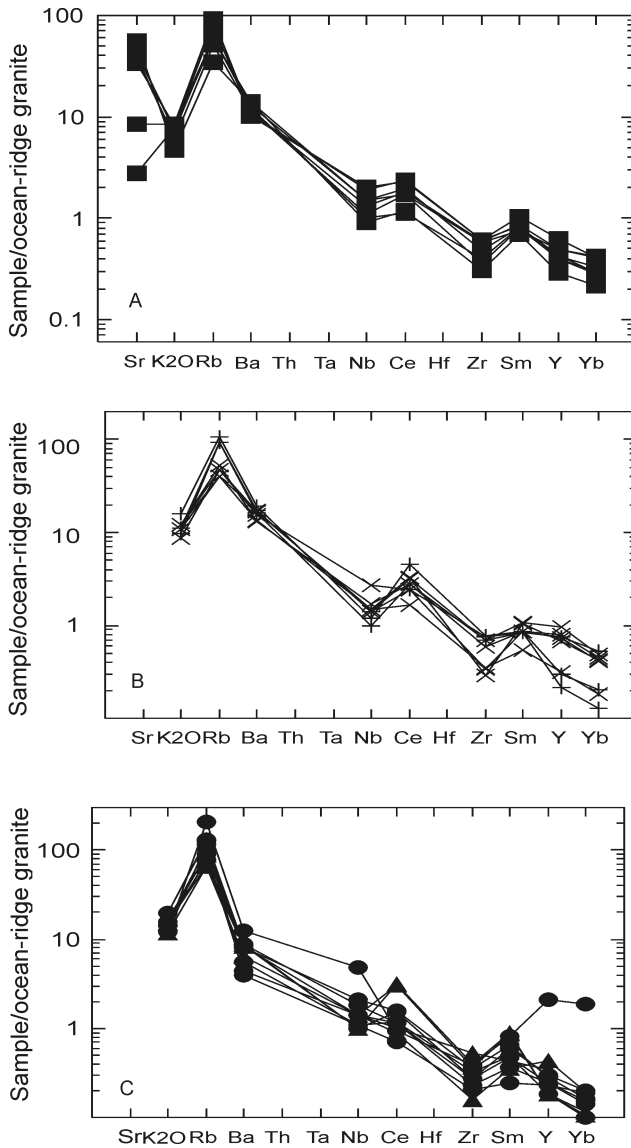


FIG. 8. Spidergrams normalized against ORG values after Pearce et al. (1984), for granitoids from Rio dos Bugres Mine association: A. Dioritic rocks. B. Granitoids. C. Tonalitic rocks.

granites with fluorite, which can be used as criteria for fluorite prospecting. REE patterns with sharply negative Eu anomalies and CeN/YbN ratios close to 1 are typical of albitized granites and albitites.

Acknowledgments

This research had financial support from CAPES-COFECUB and CNPq.

REFERENCES

- Anderson, J. L., and Smith, D., 1995, The effects of temperature and fO_2 on the Al-in-hornblende barometer: *American Mineralogist*, v. 80, p. 549–559.
- Bastos Neto, A. C., Touray, J. C., and Dardenne, M. A., 1996, Géochimie isotopique (δD) appliqué à l'étude des inclusions fluides de la fluorine du district de Santa Catarina (Brésil): une discussion sur l'origine des solutions mineralisées: *Anais da Academia Brasileira de Ciências*, v. 68, p. 213–221.
- Batchelor, R. A., and Bowden, P., 1985, Petrogenetic interpretation of granitoid rock series using multicationic parameters: *Chemical Geology*, v. 48, p. 43–55.
- Bitencourt, M. F., and Nardi, L. V. S., 1993, Late to Post-collisional Brasiliano granitic magmatism in southernmost Brazil: *Anais da Academia Brasileira de Ciências*, v. 65 (sup. 1), p. 3–16.
- Bitencourt, M. F., and Nardi, L. V. S., 2000, Tectonic setting and sources of magmatism related to the Southern Brazilian Shear Belt: *Revista Brasileira de Geociências*, v. 30, p. 184–187.
- Bitencourt, M. F., and Nardi, L. V. S., 2004, The role of xenoliths and flow segregation in the genesis and evolution of the Paleoproterozoic Itapema Granite, a crustally derived magma of shoshonitic affinity from southern Brazil: *Lithos*, v. 73, p. 1–19.
- Bowden, P., and Kinnaird, J. A., 1984, The petrology and geochemistry of alkaline granites from Nigeria: *Physics of the Earth and Planetary Interiors*, v. 35, p. 199–211.
- Debon, F., Le Fort, P., and Sabat, P., 1988, Uma classificação química-mineralógica das rochas plutônicas comuns, e suas associações, método e aplicações: *Revista Brasileira de Geociências*, v. 18, p. 122–133.
- Droop, G. T. R., 1987, A general equation for estimating Fe^{+3} concentrations in ferromagnesian silicates and oxides from microprobe analyses, using stoichiometric criteria: *Mineralogical Magazine*, v. 51, p. 431–435.
- Flores, J. A., 1998, Mineralogia e geoquímica das alterações metassomáticas e hidrotermais das rochas encaixantes da mineralização de fluorita da mina Rio dos Bugres, Santa Catarina, Brasil: Unpubl. Ph.D. thesis, Universidade Federal do Rio Grande do Sul, Porto Alegre, Brasil, 245 p.
- Fragoso-César, A. R. S., Wernick, E., and Soliani Jr., E., 1982, Associações petro-tectônicas do Cinturão Dom Feliciano (SE da Plataforma Sul-Americana), in XXXII Congresso Brasileiro de Geologia, Sociedade Brasileira de Geologia, 1982, *Anais*, v. 1, p. 1–12.
- Jelinek, A., 2002, Evolução geológica do distrito fluorítico de Santa Catarina: Estudo integrado de mineralogia, geoquímica e termotectônica por traços de fissão em apatita: Unpubl. Ph.D. thesis, Universidade Federal do Rio Grande do Sul, Porto Alegre, Brazil, 205 p.
- Leake, B. E., Wooley, A. R., Arps, C. E. S., Birch, W. D., Gilbert, M. C., Grice, J. D., Hawthorne, F. C., Kato, A., Kisch, H. J., Krigovichev, V. G., Linthout, K., Laird, J., Mandarino, J., Maresch, W. V., Nickel, E. R., Rock, N. M. S., Schumacher, J. C., Smith, D. C., Stephenson, N. C. N., Ungaretti, L., Whitaker, E. J. W., and Youzhi, G., 1997, Nomenclature of amphiboles: Report of the Subcommittee on Amphiboles of the International Mineralogical Association Commission on New Minerals and Mineral Names: *Mineralogical Magazine*, v. 61, p. 295–321.
- Le Maitre, R. W., 1989, A classification of igneous rocks and glossary of terms: Oxford, UK, Blackwell, 193 p.
- Liégeois, J. P., 1998, Preface—some words on the post-collisional magmatism: *Lithos*, v. 45, p. xv–xvii.
- Middlemost, E. A. K., 1994, Naming materials in the magma/igneous rock system: *Earth Science Review*, v. 37, p. 215–224.
- Nachit, H., Razafimahefa, N., Stussi, J. M., and Carron, J. P., 1985, Composition chimique des biotites et typologie magmatique des granitoides: *Compt Rendus d'el Academie des Sciences de Paris*, v. 301, no. 11, p. 813–818.
- Nardi, L. V. S., 1991, Caracterização petrográfica e geoquímica dos granitos metaluminosos da associação alcalina: *Revisão: Pesquisas*, v. 18, no. 1, p. 44–57.
- Nardi, L. V. S., and Bonin, B., 1991, Post-orogenic and non-orogenic alkaline granite associations: The Saibro Intrusive Suite, southern Brazil. A case study: *Chemical Geology*, v. 92, nos. 1/3, p. 197–212.
- Nardi, L. V. S., and Lima, E. F., 2000, Hybridisation of mafic microgranular enclaves in the Lavras Granite Complex, southernmost Brazil: *Journal of South American Earth Science*, v. 13, p. 67–78.
- Patiño Douce, A., 1995, Experimental generation of hybrid silicic melts by reaction of high-Al basalt with metamorphic rocks: *Journal of Geophysical Research*, v. 100, p. 15,623–15,639.
- Patiño Douce, A., 1999, What do experiments tell us about the relative contributions of crust and mantle to the origin of granitic magmas?, in Castro, A., Fernandez, C., and Vigneresse, J. L., eds., *Understanding granites: Integrating new and classical techniques*: Geological Society, London, Special Publications, v. 168, p. 55–75.
- Pearce, J., 1996, Sources and settings of granitic rocks: *Episodes*, v. 19, no. 4, p. 120–125.
- Pearce, J. A., Harris, N. B. W., and Tindle, A. G., 1984, Trace element discrimination diagrams for the tectonic interpretation of granitic rocks: *Journal of Petrology*, v. 25, p. 956–983.
- Peate, D. W., Mantovani, M. S. M., and Hawkesworth, C. J., 1988, Geochemical stratigraphy of the Paraná continental flood basalts: Borehole evidence: *Revista Brasileira de Geociências*, v. 18, p. 212–221.
- Sallet, R. G., 1988, Etude pétrologique et métallogénique d'un secteur du district à fluorine de Santa Catarina, Brésil. Les granitoides précambriens monzonitiques source probable de la fluorine post-jurassique:

- Unpubl. Ph.D. thesis, Université, Paris VI, Paris, France, 233 p.
- Sommer, C. A., Lima, E. F., Nardi, L. V. S., Liz, J. D., and Waichel, B. L., 2005, The Neoproterozoic mildly alkaline bimodal volcanism in southern Brazil: Geological and geochemical Aspects: *International Geology Review*, v. 47, 2005, in press.
- Sun, S. S., 1982, Chemical composition and origin of the Earth's primitive mantle: *Geochimica et Cosmochimica Acta*, v. 46, p. 179–192.
- Tassinari, C. G., and Flores, J. A., 1992, Aplicação dos isótopos Sr e Nd na mineralização de fluorita do poço 5, Segunda Linha Torrens, sudeste de Santa Catarina, *in* Congresso Brasileiro de Geologia, v. 37, São Paulo, Brasil, Anais, v. 1, p.259–269.
- Thompson, R. N., Morrison, M. A., Hendry, G. L., and Parry, S. J., 1984, An assessment of the relative roles of crust and mantle in magma genesis: An elemental approach: *Philosophical Transactions of the Royal Society of London*, v. A 310, p. 549–590.
- Velde, B., 1985, Clay minerals: A physico-chemical exploration of their occurrence: Amsterdam, The Netherlands, Elsevier, 425 p.
- Whalen, J. B., Currie, K. L., and Chappell, B. W., 1987, A-type granites: Geochemical characteristics, discrimination, and petrogenesis: *Contributions to Mineralogy and Petrology*, v. 95, p. 407–419.